

# Sub-slab mantle flow parallel to the Caribbean plate boundaries: Inferences from SKS splitting

L.T. Piñero-Feliciangeli <sup>a</sup>, J.-M. Kendall <sup>b,\*</sup>

<sup>a</sup> Instituto de Ciencias de la Tierra, Universidad Central de Venezuela, Caracas, Venezuela

<sup>b</sup> Department of Earth Sciences, University of Bristol, UK

## ARTICLE INFO

### Article history:

Received 16 January 2007

Received in revised form 22 January 2008

Accepted 22 January 2008

Available online 22 August 2008

### Keywords:

Anisotropy

Caribbean

Shear-wave splitting

Mantle geodynamics

Plate tectonics

## ABSTRACT

Upper-mantle deformation near the margins of the Caribbean plate is investigated using observations of shear-wave splitting in teleseismic and local shear phases. The Caribbean plate is almost stationary in the hot-spot reference frame and is wedged between the North America, South America, Nazca and Cocos plates; collisional belts and major shear zones encircle the plate. Data from seismic stations operated by IRIS, GEOSCOPE, the Venezuelan Seismological Network, and the British Geological Survey have provided nearly 2000 seismic records for analysis. Analysis of shear-wave splitting in teleseismic core phases (e.g., SKS) at stations reveals fast shear-wave polarisations that are conformal to the plate boundary, paralleling the major structural features. The magnitude of the splitting is in general quite large (1.2–2.1 s). In northern Venezuela, the magnitude of splitting increases towards the Caribbean–South American collisional front. Local shear phases from earthquakes up to 200 km deep beneath northeastern Venezuela show very small amounts of splitting (0.1–0.3 s). Analysis of the depth dependence in the magnitude of the splitting suggests that most of the upper-mantle wedge is isotropic and the splitting in the local phases is mostly accrued in the crust and uppermost mantle. In NE Venezuela fast shear-wave polarisations in both the local and teleseismic phases closely parallel the fault systems in the region, suggesting that the crust and mantle are coupled in this area. Stations on the Island of Montserrat and near Bucaramanga, Columbia, also show very small magnitudes in local S-wave splitting, but large amounts of SKS splitting. In general, the small magnitude of the local S-phase splitting suggests that the teleseismic phases accrue considerable splitting beneath the top of the slab. We interpret the bulk of the splitting in terms of sub-slab flow that is forced around the Caribbean plate due to the convergence of the surrounding plates.

© 2008 Elsevier B.V. All rights reserved.

## 1. Introduction

The Caribbean region and its plate boundary zones provide a natural laboratory to study many different tectonic environments. The present day plate margin corresponds to variably-wide deformation belts of Mesozoic–Tertiary age. The western and eastern margins consist of collisional systems with variously evolved magmatic arcs (Central American Isthmus, Lesser Antilles). The northern and southern margins are marked by major shear zones (Montagua Belt in Guatemala, Greater Antilles, Northern Venezuela Cordilleras). Two different views of the tectonic evolution of the Caribbean are of interesting debate. One hypothesis proposes an allochthonous (Pacific) origin of the Caribbean (Alvarez, 1982; Pindell, 1985; Pindell and Barret, 1990). The other suggests an in-situ origin in an intra-plate setting between the two Americas (Meschede and Frisch, 1998). Knowledge of the structure and flow patterns of the mantle below the

Caribbean region is of crucial importance to understanding the geodynamics of the region, and will offer insight into its tectonic development. Central to this is the relation between the mantle lithosphere and crustal features, and the relationship of deeper mantle flow to Caribbean plate motion. In this work, we address some of these issues by investigating the seismic anisotropy and, hence, style of crust and mantle deformation in the region.

Studies of seismic anisotropy provide insights into past and present dynamic processes within the solid Earth, including those associated with mantle convection, the formation and destruction of tectonic plates, and orogeny. Shear-wave splitting is a tell-tale signature of such anisotropy. On entering an anisotropic medium, two shear waves will propagate with polarisations approximately orthogonal to each other and with different velocities. The difference in arrival times between the two quasi-S waves is known as shear-wave splitting or birefringence. The orientation of the shear wave provides constraints on the elastic symmetry of the medium and the delay time between the two shear waves is an indicator of the magnitude of the anisotropy. These parameters, polarisation and delay time, offer insights into deformation processes.

\* Corresponding author.

E-mail addresses: [pinerolaura@gmail.com](mailto:pinerolaura@gmail.com) (L.T. Piñero-Feliciangeli), [gljmk@bristol.ac.uk](mailto:gljmk@bristol.ac.uk) (J.-M. Kendall).

Numerous mechanisms can cause seismic anisotropy, but they all reflect underlying order within a medium. In the mantle, anisotropy is most commonly attributed to the preferred alignment of crystals due to plastic deformation or lattice preferred orientation (LPO). Olivine is the most common mantle mineral in regions shallower than roughly 410 km and shows most pronounced LPO when deformation is accommodated via dislocation glide. A large number of factors control the LPO development, including grain size, presence of fluids, strain rate and temperature. Most mantle peridotites show significant olivine LPO (Mainprice et al., 2000), where most commonly the *a*-axis aligns with the shear direction. However, the presence of water can lead to different texture patterns and strengths. For example, in regions of high water content and high stress, the *c*-axes of olivine crystals will align sub-parallel to the shear direction (Jung and Karato, 2001). This so-called B-type fabric may be present in parts of the mantle wedge in subduction zones (Kneller et al., 2005).

Alternatively, a preferred orientation of inclusions, or shape-preferred orientation (SPO), can be very effective in generating anisotropy. The alignment of fracture sets or thin vertical cracks is thought to be the dominant mechanism for anisotropy in the crust (Crampin, 1984; Silver, 1996). Compositional layering, where there is a strong contrast in elastic stiffness between layers, is another SPO mechanism (Backus, 1962). Within the mantle, the preferred alignment of ellipsoidal melt inclusions in rift settings can generate significant amounts of anisotropy (Kendall, 1994; Kendall et al., 2005). It is conceivable that such melt-related mechanisms may be at play in subduction regions.

Here we investigate shear-wave splitting beneath the Caribbean region; this will allow us to evaluate the seismic anisotropy structure in this area and offer insight into lithospheric anisotropy and the dominant style of mantle flow in the region. There are a number of challenges in interpreting observations of seismic anisotropy in the upper mantle beneath the Caribbean as many mechanisms will be at play. Many factors control anisotropy at plate boundaries (Blackman and Kendall, 2002). Viscous coupling between the plates and convecting mantle will effectively generate olivine LPO. The plates themselves will preserve the signature of anisotropy inherited at the time of their formation. The presence of melt and water may generate different styles of anisotropy in the upper-mantle wedge (e.g., melt-induced SPO or B-type fabric). Finally, deformation at the various plate boundaries in the Caribbean will modify the fossil lithospheric anisotropy. Cumulatively, these mechanisms will lead to multiple layers of anisotropy, evidence of which is revealed by directional dependencies in apparent splitting parameters in near vertically travelling seismic phases (Silver and Savage, 1994). To address these issues we use observations of shear-wave splitting in teleseismic phases, such as SKS and SKKS, to map variations in anisotropy in the region. Where possible, this is augmented by studies of splitting in local shear phases, which can be used to further constrain depth variations in the anisotropy.

### 1.1. Tectonic setting

The Caribbean Plate represents a lithospheric fragment between four major plates: the North- and South-American, the Cocos and the Nazca Plates. It moves eastwards relative to the North American and the South American plates at a relatively slow rate of around 1–2 cm/yr (Jordan, 1975; Stein et al., 1988; DeMets et al., 1990).

More locally, at the eastern part of the Caribbean Plate boundary, the Atlantic oceanic lithosphere subducts at the Lesser Antilles Trench (see Fig. 1). The volcanic arc is Neogene in age, is about 850 km long and extends from eastern Venezuela in the south to as far north as the western Puerto Rico–Virgin Islands. Various studies of the active seismicity along the entire length of this boundary reveal a Wadati–Benioff zone extending down to a depth of 150–200 km (Stein et al., 1988; Russo et al., 1993). The average dip is 50–60° in the North and

vertical south of Grenada (Girardin and Gaulon, 1983). The subducted slab is 120 to 180 km beneath the present line of volcanic islands (Wadge and Shepherd, 1984). Tomographic images show a deeper high-velocity anomaly which has been interpreted tentatively as the remnants of Atlantic lithosphere subducted to a depth of 500 to 600 km (Van der Hilst, 1990).

At the western margin the Cocos plate subducts beneath the Caribbean plate along the Middle American Trench. This has controlled the tectonics on this part of the boundary zone developing some important structural features in the region, which include a large transform fault and deformation belts. The Panama fracture zone, which is a right-lateral transform fault, lies off the southern border of the boundary and is the boundary zone between the Cocos and Nazca Plates. The Cocos Ridge, located west of this boundary zone, is also being subducted beneath southern Costa Rica as part of the Cocos Plate. To the north of the Panama fracture zone lies a convergent margin between the Panama block and the Caribbean, called the Panama Deformation Belt. This tectonic feature extends from the Caribbean coast of Colombia to inland within Costa Rica. The Wadati–Benioff geometry at the western border of the Caribbean Plate shows a decrease in the maximum depth of earthquakes from 220 km under Nicaragua to less than 50 km under southern Costa Rica (Protti et al., 1994). In central Mexico, near the trans-Mexican Volcanic Belt, tomographic images indicate low-angle subduction structure interpreted as the subduction of the Cocos plate (Van der Hilst, 1990). The same is observed in the segment from south of Mexico to the Nicoya Peninsula near the south-westward continuation of the Hess Escarpment. In other segments of the Middle American Trench, tomographic images do not indicate the down-going Cocos Plate (i.e., beneath northern Mexico, Isthmus of Tehuantepec and Panama). The remnant subducted Farallon plate is visible and continuous across the 660 discontinuity and also visible in the lower mantle.

The northern Caribbean margin consists of a 2000 km-long series of faults that connects the Lesser Antilles trench in the east to the Middle American trench in the west (see Fig. 1). The plate motion that occurs across the predominantly east–west striking major faults is primarily left-lateral. It is a tectonically active margin characterised by intermediate crustal thicknesses, high seismicity, large Bouguer gravity and magnetic anomalies, late Cenozoic volcanic activity in central Hispaniola, and active oceanic volcanism in the Cayman trough spreading center.

In the south, the Caribbean and South American Plates interact in a wide and complex deformation zone. This region is the site of island arc accretion to a continent, a process thought to be a primary mechanism in the construction of continents. In broad terms the boundary consists of a right-lateral transpressional fault of approximately 1000 km length, connecting two trench zones at either end. At present a fold and thrust belt/foreland basin system is developing between the two subduction zones (Avé Lallemant, 1997). The north-western boundary of this zone is the result of a complex interaction between the Caribbean, South America and Nazca plates. The plate boundary in eastern Colombia and western Venezuela, consists of an active transpressional zone, 600 km wide, that extends from the northern flank of the Southern Caribbean deformation belt south-westward into the Merida Andes. The whole area comprises a set of discrete tectonic blocks which move independently among the surrounding larger plates (Caribbean, South America and Nazca) (Audemard and Audemard, 2002). The blocks are bounded by a series of faults in that region, the Oca–Ancon in the north, the Bocono in the Merida Andes and the Santa Marta–Bucaramanga fault in Colombia. The Oca–Ancon and Bocono faults are characterised by right-lateral, strike–slip motion and responsible for most of the shallow seismicity observed in this area. Two different subducting slabs are proposed in this north-western area, one of older age corresponding to Caribbean Plate subduction (Taboada et al., 2000) and the other of younger age

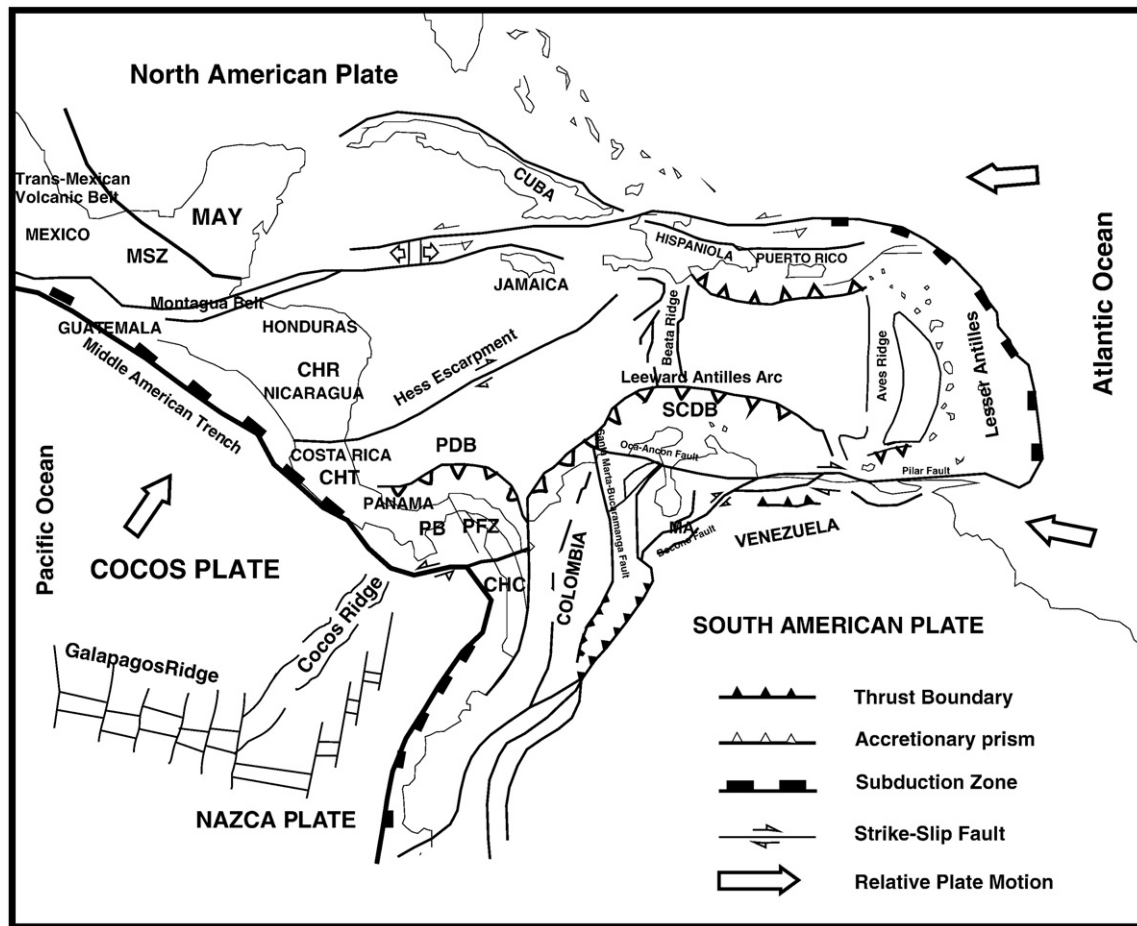


Fig. 1. Structural map of the Caribbean region (after Giunta et al., 2006). Abbreviations specify the following structural features (from top left in a counterclockwise direction): MAY—Maya block; MSZ—Montagua Suture Zone; CHR—Chortis Block; CHT—Chorotega Block; PDB—Panama Deformation Belt; PB—Panama block; PFZ—Panama fracture zone; CHC—Choco block; SCDB—Southern Caribbean Deformation Belt.

corresponding to the Leeward Antilles subduction (Audemard and Audemard, 2002). The Leeward Antilles subduction zone is a region of young, south dipping, amagmatic, oceanic subduction that started in the last 5 MA (Audemard, 2000). The slab is nearly horizontal, dipping  $16^{\circ}\text{S}$ , and is 400–450 km in length (Van der Hilst, 1990). The eastern part of the plate boundary zone is the result of a highly oblique dextral collision between the Caribbean and South American plates. The collision created a transpressive orogenic belt which can be divided, from north to south, into (Avé Lallemant, 1997): a) the Southern Caribbean deformation belt; b) the Leeward Antilles volcanic arc; c) the Cordillera de la Costa belt; d) the Serrania del Interior foreland fold and thrust belt. There is both geologic and seismic evidence of dextral strike-slip, compressional, and extensional motions consistent with deformation in a transpressive dextral simple shear environment. Tomography studies in the north-eastern Venezuela and Trinidad show an unusual structure below this region (VanDecar et al., 2001). A relatively high-velocity (minimum 2%) anomaly trends WSW from the seismically defined Lesser Antilles slab beneath and NW of the Paria Peninsula to a point below the Venezuelan Serrania del Interior. This feature has been interpreted as part of the detached or detaching subducted oceanic South American slab. A minimum in the Bouguer gravity field in a continental setting, which does not correlate well with topographic features, is explained by the presence of low-density slab material at depth (VanDecar et al., 2001).

One of the aims of our work is to establish what correlation patterns of shear-wave splitting, and hence anisotropy, have with these large-scale tectonic features.

## 1.2. Previous studies of SKS splitting in the region

A compilation of previous shear-wave splitting measurements at stations in the Caribbean region is summarised in Table 1. SJG, located near the North America–Caribbean (Na–Ca) plate boundary zone, shows an average fast shear-wave polarisation direction nearly parallel to the plate boundary (east–west) and an accumulated delay time of 1.2 s (Russo et al., 1996). Similarly, average fast polarisation directions for SKS phases

Table 1  
Previous shear-wave splitting studies at the Caribbean seismic stations

Station	Latitude	Longitude	$\phi$ ( $^{\circ}$ )	$\delta t$ (s)	Source
BARV	10.660	-63.170	$84 \pm 2$	$2.1 \pm 0.2$	(Russo et al., 1996)
CECV	10.570	-64.170	$84 \pm 2$	$1.6 \pm 0.2$	(Russo et al., 1996)
ECPV	9.180	-65.250	$83 \pm 4$	$1.0 \pm 0.2$	(Russo et al., 1996)
HSPV			$108 \pm 5$	$1.3 \pm 0.1$	(Russo et al., 1996)
MNVV	9.950	-64.030	$-79 \pm 3$	$1.6 \pm 0.2$	(Russo et al., 1996)
RSLV	10.650	-62.250	$86 \pm 3$	$1.9 \pm 0.3$	(Russo et al., 1996)
SJG	18.110	-66.150	$85 \pm 1$	$1.2 \pm 0.2$	(Russo et al., 1996)
TRNV	10.650	-61.000	$95 \pm 11$	$1.9 \pm 0.2$	(Russo et al., 1996)
BOCO	4.590	-74.043	20	1.2	(Vinnik et al., 1992)
BUCA	6.800	-73.167	$6 \pm 15$	$0.3 \pm 0.03$	(Shih et al., 1991)
CAY	4.948	-52.317	$119 \pm 5$	$0.69 \pm 0.05$	(Barruol and Hoffmann, 1999)
CAY	4.948	-52.317	100	–	(Vinnik et al., 1989)
CAY	4.948	-52.317	119	0.7	(Russo and Silver, 1994)
UNM	19.329	-99.178	$26 \pm 5$	$1.10 \pm 0.14$	(Barruol and Hoffmann, 1999)
KOG	5.207	-52.732	$-50 \pm 3$	$0.84 \pm 0.10$	(Barruol and Hoffmann, 1999)

$\phi$  refers to the polarisation azimuth of the fast shear wave,  $\delta t$  refers to the time delay between fast and slow shear wave.

**Table 2**  
Broad-band 3 component seismic stations used in this study

Code	Site	Latitude (°N)	Longitude (°N)	Period
SDV	Santo Domingo, Venezuela	08.8863	-70.626	1993–2003
JTS	Juntas de Abangares, Costa Rica	10.291	-84.9520	1993–2003
SJG	San Juan de Puerto Rico, USA	18.112	-66.1500	1993–2003
BOCO	Bogota, Colombia	04.5870	-74.043	1993–2000
FDF	Fort de France, Martinique	14.735	-61.143	1993–2000
HDC	Heredia, Costa Rica	10.027	-84.117	1995–2000
MBRY	Montserrat	16.704	-62.153	1997–2000
MBBE	Montserrat	16.744	-62.160	1997–2000
MBGB	Montserrat	16.732	-62.228	1997–2000
MBGH	Montserrat	16.723	-62.208	1997–2000
MBBY	Montserrat	16.698	-62.203	1997–2000
GUNV	Guanoco, Venezuela	10.162	-62.943	2000
GUIV	Guiría, Venezuela	10.6470	-62.223	2001–2003
CRUNV	Guiría, Venezuela	10.6167	-63.183	2002–2003
BAUV	El Baul, Venezuela	8.9434	-68.042	2003

The station code, site, latitude, longitude and time period of data analysed are indicated.

at all stations located in the northeastern part of Venezuela (BARV, CECV, ECPV, HSPV, MNVV, RSLV and TRNV), trend nearly east–west, parallel to Caribbean–South America (Ca–SA) plate boundary (Russo et al., 1996). Delay times from several stations are near or over 2 s; these values are among the highest reported globally (Silver, 1996). Station BOCO lies in Columbia, and a single previous SKS measurement shows 1.2 s of splitting and reveals a fast shear-wave polarisation that parallels the nearby the Bocono fault (Vinnik et al., 1992). In a nearby region, results from local events at 9 stations (collectively referred to as BUCA) show a similar average fast polarisation direction of  $N6^{\circ}E \pm 15^{\circ}$  (Shih et al., 1991), but much smaller splitting times. Most of the events originated in the so-called Bucaramanga nest, which lies roughly 160 km beneath the eastern Andes. Delay times for the different stations in this region range from  $(0.19 \pm 0.03)$  s to  $(0.42 \pm 0.04)$  s, where a clear trend of increasing time delay with increasing events depth was observed. Barruol and Hoffmann (1999) determined shear-wave splitting results from stations CAY, KOG, and UNM, all part of the Geoscope network. UNM lies in Mexico away from the Caribbean plate boundary. Teleseismic results at stations CAY and KOG, which are both located in a passive margin regime in French Guyana, showed delay times less than 1 s. Studies by Vinnik et al. (1989) and Russo and Silver (1994) found similar results at station CAY.

## 2. Dataset

Shear-wave splitting analysis for local and teleseismic events were studied at different stations in the Caribbean Region: four stations of

the IRIS Global Seismic Network (SDV, JTS, SJG and BOCO), four from the Venezuelan Seismological Network operated by Funvisis (GUNV, CRUNV, GUIV, BAUV), five run by the British Geological Survey (BGS) in Montserrat and two run by Geoscope Seismic Program Network (FDF, HDC). All stations are broad-band three component stations. The exact locations, time period for data analysis, and other relevant information about the stations are given in Table 2.

We selected clear recordings of teleseismic SKS, SKKS and local S phases for shear-wave splitting analysis (Fig. 2). For SKS and SKKS phase analysis, events with epicentral distances between  $85^{\circ}$  to  $135^{\circ}$  and magnitudes greater than  $M_b = 5.8$  were chosen. The selection of S phases was restricted to events with raypaths within the critical angle of  $\sim 35^{\circ}$  to the vertical. This selection is done in order to avoid distortion in both amplitude and shape of the S phase recorded due to post critical S-to-P reflections generated at and near the free surface (Crampin and Booth, 1985).

In total about 2000 earthquakes-station recordings were examined in this study. In general, noise levels are high at most of the stations used in this study due to their proximity to the coast (many are island stations). Events were analysed only if they showed a good S–N ratio and a clear arrival of the relevant shear-phase. Filtering was applied to improve the S–N ratio of the events. For teleseismic phases (e.g., SKS) a Butterworth bandpass filter with corner frequencies of 0.01 Hz and 0.3 Hz and 2 poles, was applied in 2 passes. For the case of local S phases we applied a Butterworth bandpass filter with corner frequencies of 1 Hz and 3 Hz (again 2 poles in 2 passes) in order to remove high frequency noise.

## 3. Data processing

### 3.1. Shear-wave splitting analysis

In an isotropic Earth the particle motion of P-waves will be aligned with the direction of energy transport, but the S-wave particle motion can be in any direction in the plane perpendicular to the direction of wave propagation. In anisotropic media the P-wave particle motion is no longer aligned with the ray direction and two independent shear waves propagate with polarisations fixed by the symmetry of the anisotropy. Anisotropy is commonly characterised by measuring the polarisation of the leading shear wave, the ‘fast’ direction ( $\phi$ ), and the relative arrival-time delay ( $\delta t$ ) of the trailing (‘slow’) shear wave. The method for measuring shear-wave anisotropy (or shear-wave splitting) used in this study is based on Silver and Chan (1991). We analyse both teleseismic core phases (SKS and SKKS) and S phases from local events. Studies of both local and teleseismic events can be used to study variations in

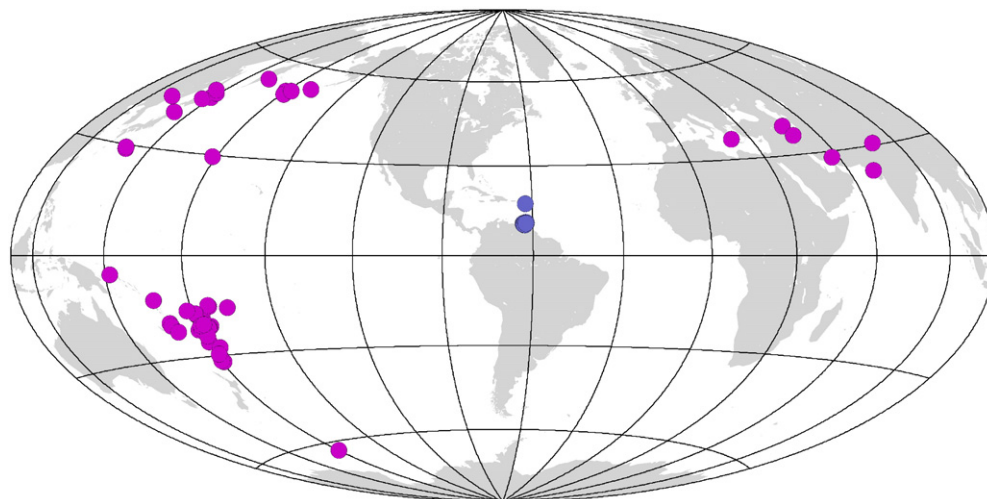


**Fig. 2.** Teleseismic (purple) and local (blue) events used to study shear-wave splitting beneath the Caribbean region. (For interpretation of the references to color in this figure legend, the reader is referred to the web version of this article.)

anisotropy as a function of depth (e.g., Gledhill and Stuart, 1996; Fouch and Fischer, 1996).

Shear-wave splitting measurements from core phases such SKS and SKKS phases have become very popular because the anisotropy can be confined to the mantle path below the receiver. These waves begin as S-waves, are converted to P-waves at the boundary with the liquid outer core, and are converted back to S-waves when they return into the mantle. In an isotropic 1D Earth the transmitted wave is polarised in the vertical–radial plane at the core–mantle boundary and SKS energy should not be observed on the transverse component. The seismograms can be therefore rotated and time shifted in order to eliminate the energy from the transverse component (i.e., remove the effect of anisotropy) and thus linearise the S-wave particle motion. However, in an Earth with 3D structure the SKS (or SKKS) phases may not be initially polarised in the saggital plane. More generally, the particle motion can be linearised by finding the rotation and time shift which minimizes the second eigenvalue of the covariance matrix constructed from the horizontal components.

For mantle S phases, the initial polarisation is not known and we must always estimate the splitting parameters ( $\phi$  and  $\delta t$ ) by mini-

minising the smaller eigenvalue of the two-dimensional covariance matrix. One of the most important problems that has to be considered in the analysis of any S phase is that post critical S-to-P reflections at and near the free surface can generate distortions in both the amplitude and the phase of the recorded wave, thus producing a non-linear particle motion than can be mistakenly interpreted as anisotropy. In order to mitigate this problem the incidence angle at the surface must be within the critical angle, which is approximately  $35^\circ$  from the vertical (Crampin and Booth, 1985).

One example of the splitting analysis on a teleseismic SKS arrival at station SDV is shown in Fig. 3. These plots show how shear-wave splitting parameters are obtained ( $\phi$  and  $\delta t$ ). Note that the particle motion is successfully linearised and that the energy on the transverse component is minimised. A splitting result for one of the local phases analysed at station GUIV, located in the most northern eastern part of Venezuela, is shown in Fig. 4. The window selected for the analysis brackets the onset of the direct S phase arrival. The obtained shear-wave splitting parameters ( $\phi$  and  $\delta t$ ) are reasonably well constrained, the particle motion successfully linearised, and the fast and slow shear waves are well aligned after the correction.

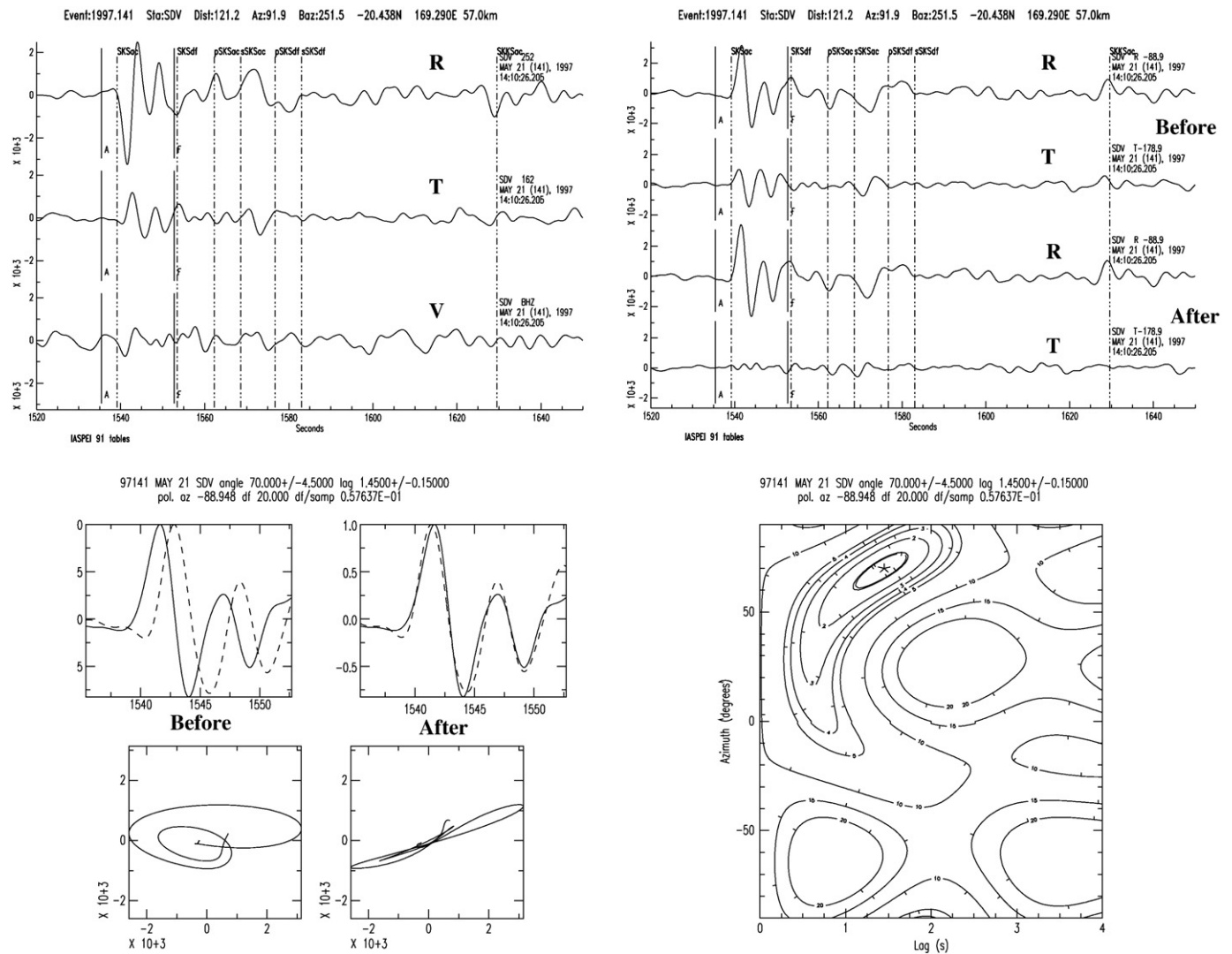


**Fig. 3.** Example of an SKS splitting result for station SDV, Venezuela. Left-top: Radial, transverse and vertical component seismograms. Note window used to isolate the shear-waveform of interest. Right-top: Radial and transverse component before and after applying the inverse splitting operator. Note how well the energy on the transverse component is reduced (compare bottom trace with that second from the top). Left-bottom: Fast (solid) and slow (dashed) shear-waveforms, before and after correction for anisotropy induced splitting (top) and corresponding particle motion diagrams (bottom). Note how the splitting correction linearises the particle motion. Right-bottom: Contour plot of energy on the corrected transverse component. The best solution is the one giving minimum energy on the transverse component, indicated by the star within the double thickness contour (the 95% confidence contour).

Splitting parameters that exhibit a lack of dependence on station-to-source backazimuth indicate wave propagation through a HTI medium (hexagonal symmetry with a horizontal symmetry axis). A dependence on backazimuth can indicate either multiple layers of anisotropy or a dipping symmetry axis. The former leads to a 90° periodicity in splitting parameters as a function of backazimuth, whilst the latter produces a 180° periodicity (Savage, 1999). However, this requires a distribution of events with good backazimuth coverage, which unfortunately, in general, is lacking for Caribbean stations.

4. Results

4.1. Teleseismic events

4.1.1. Station SDV

A total of 22 SKS and 5 SKKS signals gave acceptable splitting results at station SDV in Venezuela. All but one of the fast polarisation

directions ( $\phi$ ) lie in the range between 38° and 86°. Average results for this station, calculated using the stacking technique of Wolfe and Silver (1998), are  $(60.7 \pm 8.0)^\circ$  for  $\phi$  and  $(1.51 \pm 0.33)$  s for  $\delta t$ . Fig. 5 shows variations in  $\phi$  and  $\delta t$  with the station-to-source backazimuth. The results show little obvious variation with backazimuth and, hence, little evidence for multi-layer anisotropy, but it is difficult to be conclusive given the limited backazimuth coverage.

4.1.2. Station SJG

Station SJG in Puerto Rico produced 14 good quality SKS and 6 SKKS and 5 teleseismic S results. We also included 12 teleseismic results obtained by Russo et al. (1996). Values of  $\phi$  range between 35° and 159°, although a clear dominant E–W trend is evident.  $\delta t$  values range from null measurements (no splitting at all) to 2.45 s. Average stacked values for  $\phi$  and  $\delta t$  for this station are  $(90.7 \pm 9.0)^\circ$  and  $(1.29 \pm 0.27)$  s. Fig. 5 shows the variation in splitting parameters with backazimuth and reveals an apparent periodicity in the results, thus

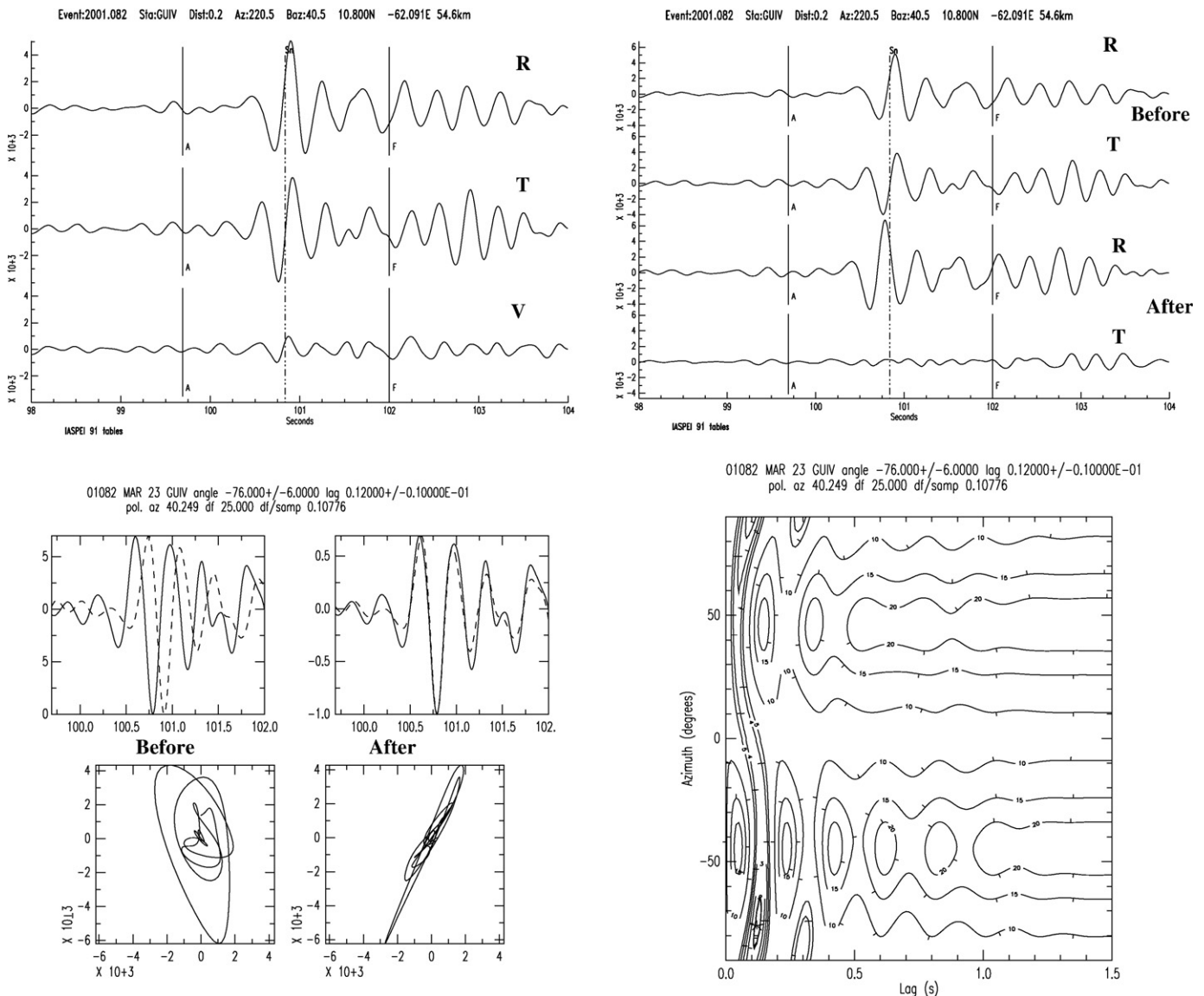


**Fig. 4.** Example of a local-S splitting results for station GUIV, Venezuela. Left-top: Radial, transverse and vertical component seismograms. Note window used to isolate the shear-waveform of interest. Right-top: The component parallel (R) and perpendicular (T) to the polarisation of the initial S phase before entering the anisotropic medium, before and after applying the inverse splitting operator. Note how well the energy on the perpendicular (T) component is reduced after the correction (compare bottom trace with that second from the top). Left-bottom: Fast (solid) and slow (dashed) shear-waveforms, before and after correction for anisotropy induced splitting (top) and corresponding particle motion diagrams (bottom). Note how the splitting correction linearises the particle motion. Right-bottom: Contour plot of energy on the corrected transverse component. The best solution is the one giving minimum energy on the transverse component, indicated by the star within the double thickness contour (the 95% confidence contour).

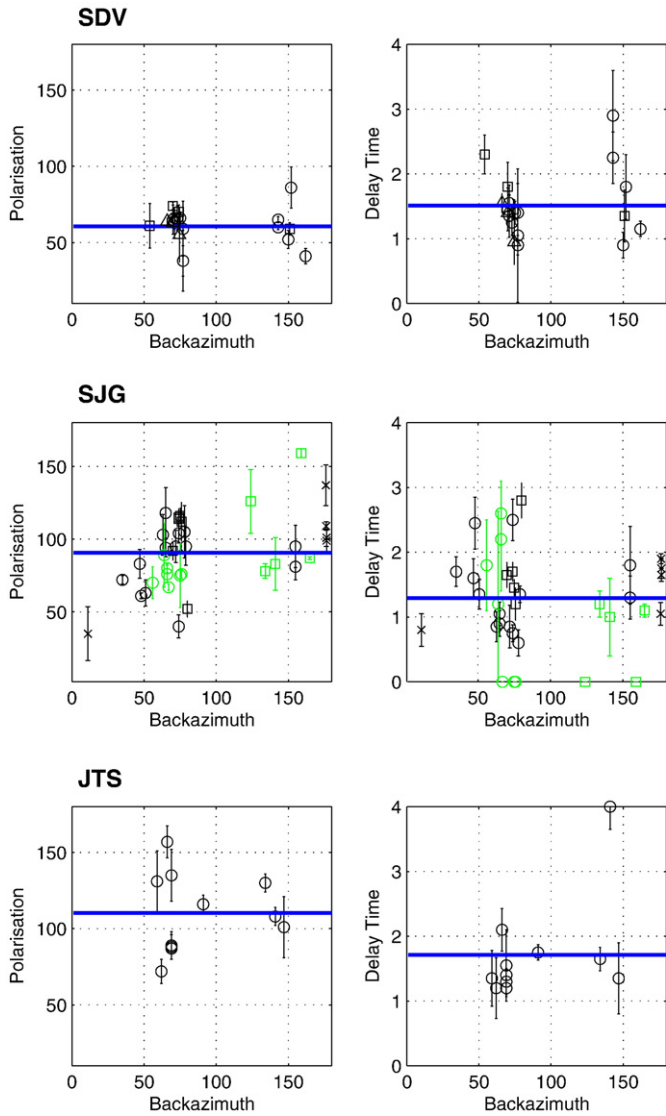


**Fig. 5.** Splitting parameters as a function of backazimuth: Top: SDV (Venezuela); Middle: SJG (Puerto Rico); Bottom: JTS (Costa Rica). Circles show results for SKS phases, squares show results for SKKS, crosses show results for teleseismic S and triangles show results for stacked data for a given backazimuth range. In the results for station SJG we included results from [Russo et al. \(1996\)](#) studies (green lines). (For interpretation of the references to color in this figure legend, the reader is referred to the web version of this article.)

suggesting multi-layer anisotropy or a dipping anisotropic symmetry axis.

#### 4.1.3. Station JTS and HDC

We obtain 9 good quality teleseismic SKS results for station JTS, and also include 2 teleseismic SKS results obtained at station HDC located about 80 km southwest of JTS. The fast shear-wave polarisation ( $\phi$ ) varies between  $72^\circ$  and  $157^\circ$ ; however, three of the better constrained results have approximately the same  $\phi$  value ( $89^\circ$ ). Values of  $\delta t$  vary between 1.2 s and 2.1 s. The average stacked values of  $\phi$  and  $\delta t$  for these station are  $(110.3 \pm 10.4)^\circ$  and  $(1.71 \pm 0.32)$  s. There appears to be little systematic variation of splitting parameters with backazimuth ([Fig. 5](#)), but more data is required to be conclusive.

#### 4.1.4. Station BOCO

In total 2 SKS and 1 SKKS results were obtained for this station, but we also include a single result obtained by ([Vinnik et al., 1992](#)), which

is consistent with our results. The stacked average values obtained using both datasets are  $(13.0 \pm 11.8)^\circ$  and  $(1.6 \pm 0.2)$  s for  $\phi$  and  $\delta t$ , respectively. There is insufficient backazimuth cover to assess evidence for multi-layer anisotropy beneath this station ([Fig. 6](#)). In a nearby region [Shih et al. \(1991\)](#) find an average fast shear-wave polarisation of  $6^\circ$  using local events from a depth of roughly 160 km, which agrees well with the teleseismic results for  $\phi$ . However, there are large discrepancies in  $\delta t$  between the splitting results for the teleseismic and local events.

#### 4.1.5. Station FDF

Station FDF, located in Martinique above the Caribbean subduction zone, had in total 7 acceptable results, 5 from SKS phases and 2 from SKKS phases. The measured values of  $\phi$  range from  $122^\circ$  to  $155^\circ$  and delay times between the fast and the slow shear wave ( $\delta t$ ) vary between 0.55 and 1.55 s. Using the [Wolfe and Silver \(1998\)](#) stacking method, the average values for  $\phi$  and  $\delta t$  are  $(136.4 \pm 16.6)^\circ$  and  $(1.186 \pm 0.627)$  s, respectively. [Fig. 6](#) shows variations with BAZ, but there are insufficient results to draw any conclusions regarding multiple layers of anisotropy.

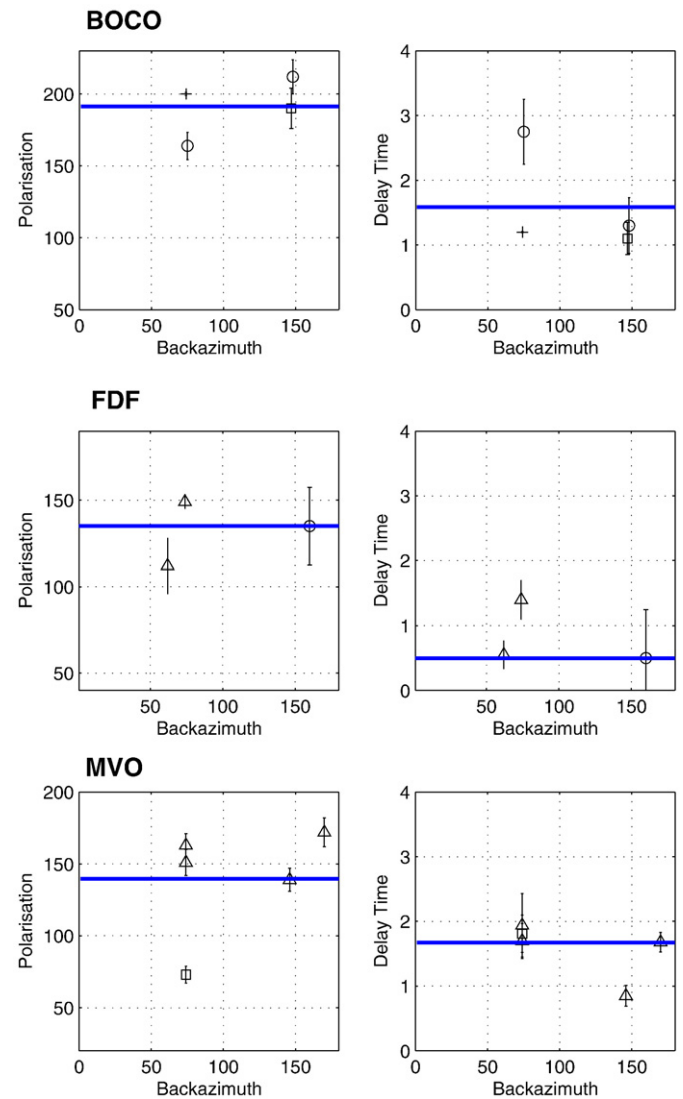


**Fig. 6.** Splitting parameters as a function of backazimuth: Top: BOCO (Columbia); Middle: FDF (Martinique); Bottom: MVO (stations on Montserrat). Circles show results for SKS phases, squares show results for SKKS, plus-signs show results from [Vinnik et al. \(1992\)](#) and triangles show results for stacked data for a given backazimuth range.

#### 4.1.6. Stations from MVO

Stations from Montserrat, located in the Lesser Antilles volcanic arc, give 7 SKS and 3 SKKS results. The values of  $\phi$  and  $\delta t$  for teleseismic phases range between  $73^\circ$  to  $179^\circ$ , and 0.66 and 2.10 s respectively. The average splitting parameters at each stations are: MBBE,  $\phi=(160.0\pm 10.0)^\circ$  and  $(2.10\pm 0.60)$  s; MBGB:  $\phi=(140.8\pm 12.3)^\circ$  and  $(1.35\pm 0.58)$  s; MBRY,  $\phi=(155.0\pm 10.0)^\circ$  and  $(1.95\pm 0.45)$  s; MBBY:  $\phi=(161.5\pm 10.0)^\circ$  and  $(1.93\pm 0.42)$  s; MBGH:  $\phi=(140.8\pm 16.33)^\circ$  and  $(1.31\pm 1.38)$  s. Average results are displayed in Fig. 7. Once again, there are an insufficient number of results to draw any conclusions about multiple layer of anisotropy from the variation in splitting parameters with backazimuth (Fig. 6).

#### 4.2. Local events

##### 4.2.1. Stations from MVO

An event 128 km deep beneath Montserrat yielded results at two stations on Montserrat. Polarisation direction and delay times for these 2 results are  $(120\pm 6.5)^\circ$  and  $(0.293\pm 0.013)$  s, and  $(154\pm 4.5)^\circ$  and  $(0.239\pm 0.013)$  s. As is observed in Fig. 7, fast polarisation directions at the two stations are consistent with polarisation directions from teleseismic phases. On the other hand delay times are very small compared to those obtained from the teleseismic events.

##### 4.2.2. Stations GUIV

The stations GUIV, GUNV and CRUNV are located in the north-eastern most part of Venezuela in the Caribbean South America plate boundary zone. In total 14 local-S phases gave acceptable splitting results at GUIV. Fast polarisation directions ( $\phi$ ) range from  $61^\circ$  to  $122^\circ$ , but the average direction of ( $\phi$ ) is approximately E–W. Values of ( $\delta t$ ) range between 0.06 and 0.14 s. The average values for  $\phi$  and  $\delta t$  obtained for station GUIV are  $(93.4\pm 7.1)^\circ$  and  $(0.106\pm 0.012)$  s, respectively. In order to characterise the anisotropic region below

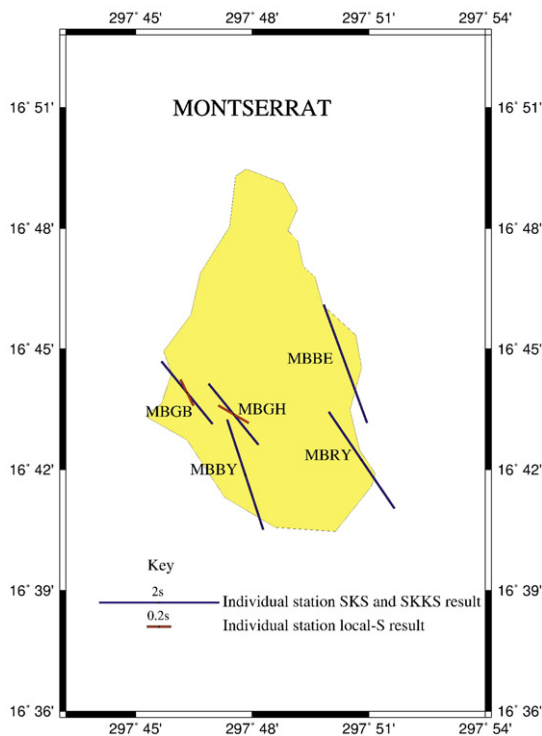


Fig. 7. Map of Montserrat showing the average splitting results at the individual stations studied. Red bars indicate results from local-S events and blue bars show those from teleseismic events. (For interpretation of the references to color in this figure legend, the reader is referred to the web version of this article.)

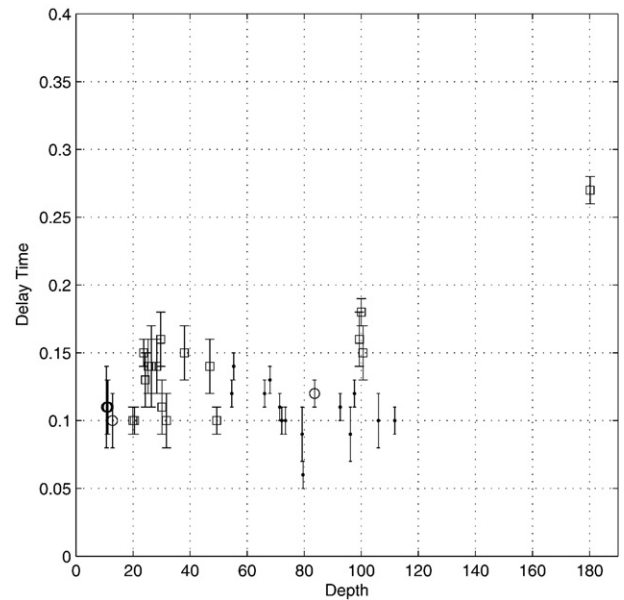


Fig. 8. Delay time versus depth for stations GUIV (dot), GUNV (square) and CRUNV (circle), located in the northeastern part of Venezuela.

the station, a plot of  $\delta t$  vs. source depth is shown in Fig. 8.  $\delta t$  is fairly constant as a function of depth, implying a shallow source of anisotropy.

##### 4.2.3. Station GUNV

This station produced 18 local-S phase results and 1 teleseismic SKS phase result. The values of  $\phi$  range between  $93^\circ$  and  $157^\circ$ . A plot of  $\phi$  vs. depth is shown in Fig. 8. The delay time ( $\delta t$ ) is fairly constant. The average values for the S phase analyses for station GUNV are  $(133.5\pm 7.2)^\circ$  and  $(0.142\pm 0.012)$  s for  $\phi$  and  $\delta t$ , respectively. A single but very well constrained SKS splitting result was obtained for this station with values  $(131.0\pm 2.5)^\circ$  and  $(1.64\pm 0.14)$  s, which agrees very well with the local S results in  $\phi$ , but not in the magnitude of the delay time.

##### 4.2.4. Station CRUNV

The results at this station are based on 5 local-S phases. Four of the five results have fast polarisation directions ( $\phi$ ) between  $123^\circ$  and  $128^\circ$ , but one well constrained result was obtained with a value of  $13^\circ$ . As with GUNV and GUIV,  $\delta t$  is fairly constant as a function of depth (Fig. 8). The average values for  $\phi$  and  $\delta t$  obtained for station CRUNV are  $(139.6\pm 9.0)^\circ$  and  $(0.110\pm 0.020)$  s respectively.

## 5. Discussion and interpretation

In general, a diverse range of tectonic processes are at work in the Caribbean region: subduction, continental orogeny and accretion, large-scale transform faults and the formation of new lithosphere at spreading centres. Despite this, if we compare the results (Fig. 9; Table 3) with the structural map of the area (Fig. 1), the fast shear-wave polarisations in the region are uniformly sub-parallel to plate boundaries.

In the northern part of our study area, the style of deformation at the NA–Ca boundary zone is characterised by a widespread sinistral shear (see Fig. 1). Station SJG lies above the Puerto Rico rigid crustal block, which is undergoing a counterclockwise rotation (Masson and Scanlon, 1991). The average fast polarisation value obtained for this station is E–W which agrees well with the surface geology of the area. However we observe considerable variability in splitting parameters at this station, which is indicative of a heterogeneous anisotropy. A logical anisotropy model to consider is one where an underlying layer is oriented in the plate motion direction and an upper layer is aligned

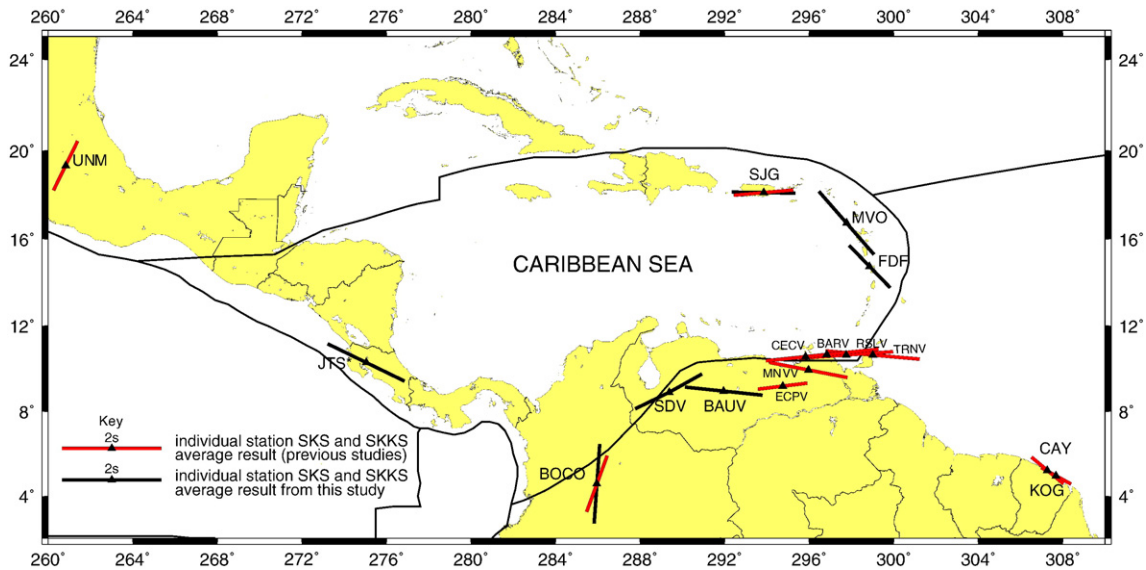


**Fig. 9.** Shear-wave splitting results at Caribbean stations derived from teleseismic phases. Thick red lines mark results from previous studies, whilst thick black lines mark results from this study. The line is oriented parallel to the polarisation direction of the fast shear wave ( $\phi$ ) and the length of the line is proportional to the magnitude of shear-wave splitting ( $\delta t$ ). Thin black lines mark plate boundaries in the region. (For interpretation of the references to color in this figure legend, the reader is referred to the web version of this article.)

with large-scale structural features, in this case the transform plate boundary between North America and the Caribbean. We model the two-layer response using the methodology of Silver and Savage (1994). Predictions from this model agree with the observations (Fig. 10), but to what degree this model is unique requires further investigation. This model implies a degree of decoupling between these two layers, but studies of S-wave splitting in local events in this region would help better constrain the depths of these two layers.

In the eastern Caribbean plate boundary zone both MVO and FDF stations show average fast polarisation ( $\phi$ ) directions parallel to the trench of the Lesser Antilles subduction zone (see Fig. 9).  $\phi$  from teleseismic phases at Montserrat are coherent with the results obtained from local S phases and both parallel the trend in subduction (Fig. 7). Teleseismic SKS and SKKS phases sample the anisotropic structure between the core–mantle boundary and the station. On the other hand S-waves from deep earthquakes within the Lesser Antilles Benioff zone traverse only the mantle wedge and crust; these phases do not sample anisotropy within and beneath the slab. Coherency in the average values of  $\phi$  from local S phases and teleseismic phases may suggest coherent deformation above and below the slab. The source depth from the local-S event analysed at 2 stations on Montserrat is 128 km. The average value of  $\delta t$  obtained for this station is 0.27 s. If we assume an average shear velocity of  $V_s = 4.5$  km/s, the percentage of anisotropy predicted in this region above the source is

an average 1.1%. In contrast, teleseismic events at Montserrat show an average of 1.68 s of splitting. Comparison with the local events implies that the bulk of the splitting ( $>1.4$  s) is accrued with the slab and the underlying mantle. Assuming a 100 km long raypath through a slab with an average S-wave velocity of 4.5 km/s would require nearly 7% anisotropy evenly distributed through the slab to explain the splitting. This could be due to fossil anisotropy frozen into the slab at its time of formation at the mid-Atlantic ridge, and the coherence in  $\phi$  within and above the slab would be coincidental. Instead it seems more likely that the deep anisotropy lies, in part, beneath the slab and the deformation above and below reflects the style of coherent along-strike mantle flow from the north around the edge of the subducting slab (see Lowman et al. (2007) for examples of such phenomena).

The eastern part of Venezuela at the Ca–SA boundary zone is an area characterised by a strong east–west trending dextral shear component and a northwest-trending compressional component. Average local-S phase results at stations GUNV, GUIV and CRUNV in this area are shown on a smaller scale map (Fig. 11); we also include results obtained from teleseismic phases from Russo et al. (1996) in this figure. Estimates of  $\phi$  from local data recorded at station GUNV, located in the most northern part, trend approximately E–W, sub-parallel to the major structural feature in the area (i.e., the El Pilar fault). This result also agrees with those of Russo et al. (1996) for splitting in teleseismic signals at the nearby station RSLV. The results for all stations located along the north coast of Venezuela (RSLV, BARV, CECV and GUIV) are approximately parallel to the average polarisation direction of the predominant foliation, fold axial planes, and brittle faulting direction in the metamorphosed sediments (Avé Lallemant and Guth, 1990). Station GUNV is located south of the major strike–slip system. Shear-wave splitting results obtained from teleseismic and local-S phases at this station are coherent with the local geology in the area. The station lies above a strike–slip fault which trends in the  $N60^\circ W$  direction. At station CRUNV the fast polarisation directions are oblique to the El Pilar fault and values obtained by Russo et al. (1996) in the nearby station BARV using teleseismic phases. Instead, they reflect more local trends in geologic features to the south of this station. In summary, in the north eastern part of Venezuela we observe continuity between teleseismic and local phases; this result suggests coupling between the crust and the mantle. Fast polarisation directions from stations located in the north eastern part of Venezuela reflect the en-echelon faulting pattern generated in this area in

**Table 3**  
Shear-wave splitting parameters for the analysed Caribbean stations

Station	Latitude	Longitude	Phase	N	$\phi \pm \Delta\phi$	$\delta t \pm \Delta\delta t$ (s)
SDV	08.8863	-70.6260	SKS, SKKS	27	$60.7 \pm 8.0$	$1.51 \pm 0.33$
JTS and HDC	10.2910	-84.9520	SKS, SKKS	11	$110.3 \pm 10.4$	$1.71 \pm 0.32$
SJG	18.1120	-66.1500	SKS, SKKS	20	$90.7 \pm 9.0$	$1.29 \pm 0.27$
BOCO	04.5870	-74.0430	SKS, SKKS	3	$13.0 \pm 11.8$	$1.6 \pm 0.2$
FDF	14.7350	-61.1430	SKS, SKKS	7	$136.4 \pm 16.6$	$1.19 \pm 0.63$
BAUV	8.9434	-68.042	SKS, SKKS	1	$-84 \pm 4$	$1.56 \pm 0.14$
MVO	16.4223	-62.0910	SKS, SKKS	10	$138.9 \pm 7.4$	$1.68 \pm 0.28$
MVO	16.4223	-62.0910	S	2	$137 \pm 6$	$0.27 \pm 0.01$
GUNV	10.162	-62.943	S	18	$133.5 \pm 7.2$	$0.14 \pm 0.01$
GUIV	10.6470	-62.223	S	14	$93.4 \pm 7.1$	$0.11 \pm 0.01$
CRUNV	10.6167	-63.183	S	5	$139.6 \pm 9.0$	$0.11 \pm 0.02$

$\phi$  refers to the polarisation of the fast shear wave,  $\delta t$  refers to the time lag between the fast and slow shear wave, and N refers to the number of successful measurements made at each station.

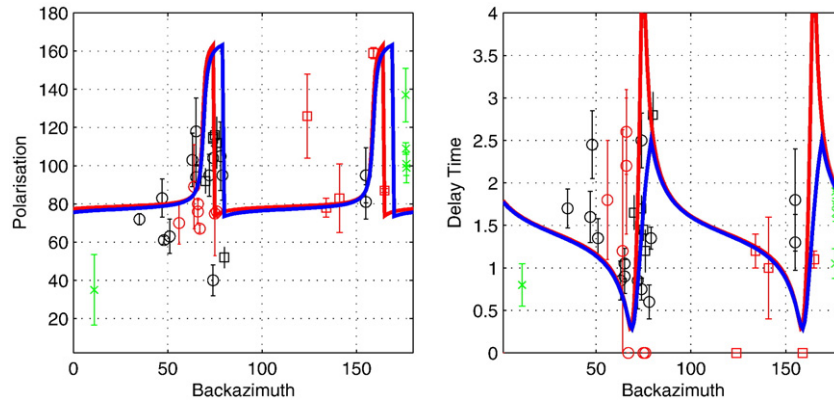


**Fig. 10.** Splitting parameters as a function of backazimuth for station SJG (Puerto Rico), including results from Russo et al. (1996) studies (green lines). Circles correspond to SKS phases, squares SKKS, and crosses to S results. Curves (solid lines) are predictions from a 2-layer model where the lower layer aligns with the direction of absolute plate motion ( $246^\circ$ ) and the upper layer aligns with the transform fault ( $270^\circ$ ). The splitting ( $\delta t$ ) is 1 s in the lower layer and 0.3 s in the upper layer. The solid red line assumes a dominant frequency of 0.1 Hz and the blue line assumes a dominant frequency of 0.2 Hz. (For interpretation of the references to color in this figure legend, the reader is referred to the web version of this article.)

response to the highly oblique dextral collision between the Caribbean and the South American plates.

The delay times from local S phases for station GUV are from events with maximum depths of 120 km. The measured delay times are quite small (0.14 s), indicating that most of the SKS splitting (1.9 s from station RSLV) lies below this depth, deep seated in the mantle. We also observe no increase in delay time with epicentral depth for this station. Similarly small values of  $\delta t$ , with no increase with depth, are observed for station CRUNV. Results for local events beneath the stations suggest little anisotropy in the mantle above the slab and the lack of depth dependence in  $\delta t$  suggests that the anisotropy may be concentrated in the crust. It also seems that delay times for teleseismic phases increase for stations located near to the Ca-SA collisional front (moving towards the El Pilar fault the splitting magnitude is: 1.0 s at ECPV, 1.3 s for HSPV, 1.6 s for MNVV, and 1.64 s; stations nearest the fault, TRNV, BARV and RSLV, show 1.9–2.1 s of splitting) (see Fig. 11). However, small amounts of splitting in

the local events indicate a deep source of anisotropy. VanDecar et al. (2001) image the edge of a detaching subducting slab in this region. The splitting contribution from deeper anisotropy could be associated with anisotropy in the slab or mantle flow around its edges. The anisotropy could be frozen into the slab, but assuming a 100 km thick slab and average S-wave velocities of 4.5 km/s, would require over 8% of anisotropy. Instead, it seems more likely that the edges of the slab and the surrounding mantle have developed a strong LPO anisotropy due to shear-stresses associated with the deviation in mantle flow around the slab edge. Such effects have been modelled in geodynamic simulations of flow around cold slab tips or edges (Lowman et al., 2007).

Results for stations SDV and BAUV are generally consistent with surface features in the area, but little is known about potential slab structure at depth in this region. Splitting at SDV is sub-parallel to the Bocono lateral strike-slip fault, which trends  $60^\circ$ NE, parallel to the Andes mountain chain.  $\phi$  at BAUV is E-W and correlates with

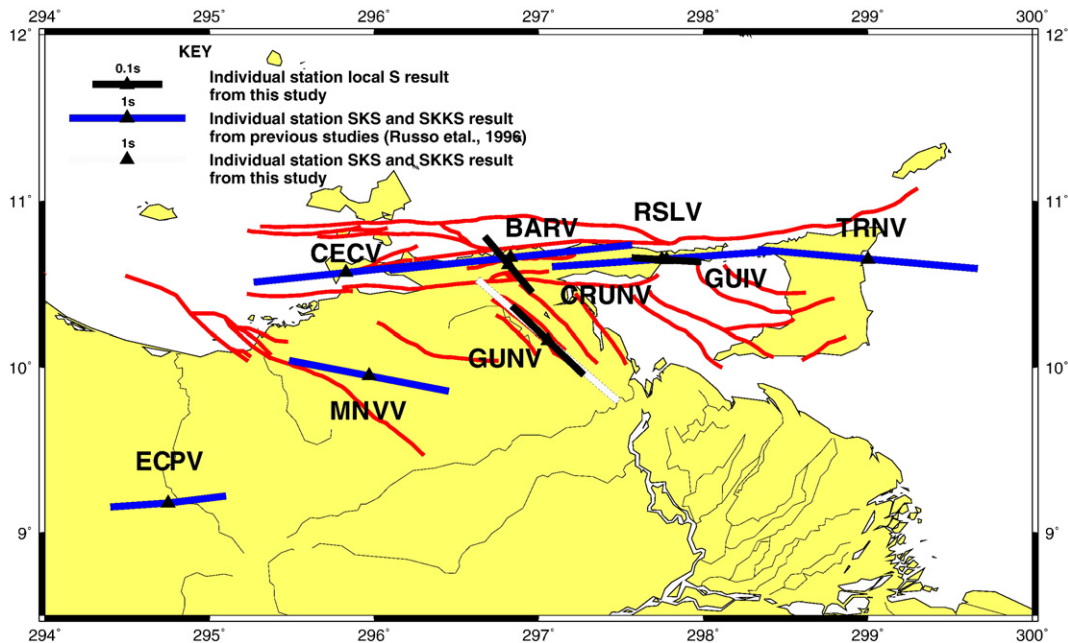


**Fig. 11.** Shear-wave splitting results from the eastern part of Venezuela. Blue bars correspond to results from (Russo et al., 1996), black bars are S phases results obtained in this study and the only white bar shows a result from a single SKS teleseismic event recorded at station GUNV. Red lines mark known fault structures in the region. (For interpretation of the references to color in this figure legend, the reader is referred to the web version of this article.)

geological features in the area (see Fig. 9). As we lack splitting results for local events at these stations, we cannot comment on the depth extent of this anisotropy or the degree of crust–mantle coupling. Further west in Columbia, BOCO and BUCA show a correlation between the orientation of anisotropy and the plate boundary. These stations are not far from each other, but the average delay time from local S phases (Shih et al., 1991) at BUCA, is 0.3 s for events at a depth of 160 km, whilst teleseismic phases at BOCO show 1.61 s. This implies that at least 1.3 s of splitting is accrued below a depth of 160 km. At face value, the consistent fast shear-wave polarisations suggest crust–mantle coupling to a considerable depth.

In the western Caribbean, results from JTS and HDC in Costa Rica are sub-parallel to the Middle American Trench. The splitting does not seem to be affected by the more E–W trending Hess escarpment or the Panama Deformation Belt (Fig. 1), but rather parallels the edge of the plate. No local events were available for these stations, so we cannot say more about depth extent of the anisotropy.

Many shear-wave splitting studies have investigated seismic anisotropy in different convergent settings around the world (see review in Park and Levin, 2002). The inferred anisotropic structures show considerable regional variability suggesting that the signal is due to a mixture of different processes. In general, asthenospheric flow in subduction regions may be driven by thermal or compositional buoyancy, by local viscous forces coupling surface and subducting plate motions to the asthenosphere, or by forces associated with larger-scale whole mantle flow. Our results for the Caribbean region show fast-shear wave polarisations aligned parallel to the plate boundaries, but we must consider potential contributions from at least 4 regions: below the slab, within the slab, in the upper-mantle wedge and within the crust.

Studies of shear-wave splitting in local events beneath subduction regions exhibit a wide range of orientations and magnitudes. Shear-wave splitting in local phases beneath Venezuela, Columbia and Montserrat show very small amounts of splitting. Similar observations have been made in other subduction regions (e.g., New Zealand (Audoine et al., 2000; Morley et al., 2006); Japan (Nakajima et al., 2006); (Kamchatka (Peyton et al., 2001)) However, large amounts of splitting are seen in other studies (e.g., Ryukyu (Long and van der Hilst, 2006); Tonga (Fischer and Wiens, 1996). Clearly not all subduction zones are equal.

Given the lack of depth dependence in the shear-wave splitting for local events beneath NE Venezuela one could conclude that the bulk of the anisotropy is accrued in the crust. The anisotropy may be due to the alignment of micro-cracks or lower crustal minerals (Crampin, 1984; Lloyd and Kendall, 2005).

Alternatively, the anisotropy could be confined to the uppermost parts of the mantle wedge. Along strike mantle flow would align the a-axes of olivine, thereby generating trench parallel splitting directions. However, the presence of water or melt might complicate this interpretation. High stresses and the presence of water can change the dominant glide system for olivine such that trench normal flow can produce trench parallel fast polarisation directions (Jung and Karato, 2001). Such B-type fabrics have been interpreted beneath the Ryukyu Arc (Long and van der Hilst, 2006). On the other hand, trench parallel fast directions could result from the preferred alignment of vertical sheets of melt aligned parallel to the slab. Holtzman et al. (2003) show that strain partitioning and melt segregation will also align olivine a-axes perpendicular to the flow direction. It is therefore conceivable that the anisotropy could be due to the combined effect of aligned melt inclusions and trench parallel aligned olivine crystals. Given the available data it is difficult to confidently decide which of these mechanisms is at play.

Teleseismic phases in the NE Caribbean boundary zone also exhibit trench parallel results, but with much larger delay times than the results for the local events. The same is true for the Montserrat stations and those in Columbia. Therefore, in these regions there must

be a deeper region of anisotropy contributing to the observed splitting in teleseismic phases. However, both water and melt-related anisotropy mechanisms are confined to the upper-mantle wedge. This leaves two plausible mechanisms for the deeper source of anisotropy: it is potentially in the slab itself or below the slab.

Tectonic plates will inherit anisotropy at their time of formation (Blackman et al., 1996), so a fossil anisotropy will be frozen into the subducting slab. Given the range of tectonic settings at the stations we have considered, one would expect the orientation of any slab anisotropy to vary with geographical position. Instead we uniformly see  $\phi$  oriented parallel to the plate boundaries. Furthermore, the magnitude of the splitting requires high amounts of anisotropy if it is confined to the slab (e.g., roughly 8% in the slab beneath northeastern Venezuela and 7% beneath Montserrat and Bucaramanga). We therefore conclude that slab anisotropy is not the dominant mechanism for the deeper source of anisotropy.

A final explanation for the deeper anisotropy is that associated with sub-slab flow. Trench parallel fast polarisation directions below the slab could be explained by mantle flow associated with slab rollback (Buttles and Olson, 1998), or toroidal flow generated by changes in the morphology and dip of the slab (Lowman et al., 2007). Buttles and Olson (1998) examined the alignment of the olivine a-axis using a laboratory analogue. They found that the rollback component of plate motion will affect mineral alignment behind the slab. Specifically in the oceanward region the alignment would be trench parallel and in the upper-mantle wedge the alignment would be subvertical. Russo and Silver (1996) argue such effects are driving along-strike flow beneath central South America. However, assessing to what degree slab rollback is at play in the Caribbean subduction zones is not straight forward. Although the Caribbean plate is migrating slowly ( $\sim 2$  cm/year), the Lesser Antilles subduction region may be experiencing rollback due its interaction with continental South America.

In a bigger context, the Caribbean plate is wedged between the converging North America, South America, Nazca and Cocos plates and one would expect mantle flow around the boundaries of the plate. The orientation of the fast teleseismic shear-wave polarisations are conformal to the plate boundary and are most probably the signature of this sub-slab flow pattern. The autochthonous or in-situ origin of the Caribbean plate model argues for an older formation of the Middle American trench ( $>200$  Ma). In contrast, the Caribbean Pacific origin model, not only proposes the migration of the Caribbean plate from the Pacific to its actual position, it also suggest a polarity reversal of subduction in this region between Aptian and Late Albian age (approx. 100 Ma). A more detailed analysis of both the heterogeneity and anisotropy beneath the western margin (Central America) is required to differentiate between these two models. Our results as they stand are consistent with ideas of the Caribbean plate being somewhat stationary with respect to the surrounding plates and mantle material flowing around the region.

## 6. Conclusions

The anisotropic structure of the Caribbean has been investigated through shear-wave splitting measurements at seismic stations in the region. Fast shear-wave polarisation directions obtained from S phases and teleseismic phases correlate well with structural features in the area. At the NA–Caribbean and Caribbean–SA boundary zones, both located in widespread shear deformation environments, fast polarisation directions align parallel to the strike–slip directions. In the Lesser Antilles volcanic arc, fast polarisation measurements are trench sub-parallel. A station near the Middle American trench also showed fast polarisation directions parallel to the trench.

Results obtained from the splitting analysis of local events up to 200 km deep beneath northeast Venezuela, Montserrat and Bucaramanga, Columbia, show small amounts of S-wave splitting and little

variation with depth. This result suggests that the anisotropy seen by the local phases is probably confined to a shallow source, possibly even the crust. The anisotropy causing the large delay times measured in teleseismic phases must be located deeper, within or below the slab.

Delay times for teleseismic phases at stations located near Ca–SA collisional front in the north eastern part of Venezuela suggest an increase in deformation moving towards the boundary. The large values of observed SKS splitting (>1.9 s) are much greater than the average value observed elsewhere around the world (Silver, 1996; Savage, 1999). This result can be linked to compression and shear associated with South America overriding its own detached oceanic slab, resulting in extreme fabric development in upper-mantle peridotites. Again, the small amounts of splitting observed in local S phases suggest that transpressional deformation in this area is deep-seated.

In parts of the Caribbean, it appears that the mantle wedge region (<200 km) is only weakly anisotropic, which suggests decoupling between the slab and the overlying mantle. The trench parallel fast shear-wave orientation may be due to the effects of water changing the dominant glide system of olivine (B-type fabric) (Jung and Karato, 2001) or may be due to the effects of aligned melt in the upper parts of the mantle wedge (Holtzman et al., 2003). However, the lack of depth dependence in the splitting results and the small magnitude of splitting suggest that anisotropy could be in fact confined to the crust.

In contrast, more variability is observed in the splitting in teleseismic phases recorded in the region. The anisotropy may be within the slab and/or below the slab. Little transition zone anisotropy is expected as transition zone minerals are nearly anisotropic or show a weakly developed LPO (Fischer and Wiens, 1996; Mainprice et al., 2000; Tommasi et al., 2004). Below the slab the trench parallel observations could be associated with mechanisms such as slab rollback (Russo and Silver, 1994; Buttles and Olson, 1998), or changes in the stress fields generated by variations in the morphology and dip of the slab (Lowman et al., 2007). In general our results suggest a connection between surface structural features and deep-seated mantle deformation.

## Acknowledgements

This research was partially funded by Consejo de Desarrollo Científico y Humanístico de la Universidad Central de Venezuela. We thank Brian Baptie for providing seismic data from the Montserrat Volcanological Observatory and the Seismological Institute of Venezuela (FUNVISIS) for making the Venezuelan data available. Andrew Frederiksen, Lucia Margheriti and 2 other anonymous reviewers are thanked for comments that have improved the presentation of the work.

## References

Alvarez, W., 1982. Geological evidence for the geographical pattern of mantle return flow and the driving mechanism of plate tectonics. *J. Geophys. Res.* 87, 6697–6710.

Audemard, F.A., 2000. Major active faults of Venezuela. 31st International Geological Congress, Rio de Janeiro, Brazil. Brazilian Geological Society (Extended abstract. CD-ROM format).

Audemard, F.E., Audemard, F.A., 2002. Structure of the Merida Andes, Venezuela: relations with the South America–Caribbean geodynamic interaction. *Tectonophysics* 301–327.

Audoine, E., Savage, M.K., Gledhill, K., 2000. Seismic anisotropy from local earthquake in the transition region from a subduction to a strike-slip plate boundary, New Zealand. *J. Geophys. Res.* 105, 7893–7908.

Avé Lallemand, H.G., 1997. Transpression, displacement partitioning, and exhumation in the eastern Caribbean/South American plate boundary. *Tectonics* 16 (2), 272–289.

Avé Lallemand, H.G., Guth, L.R., 1990. Role of extensional tectonics in exhumation of eclogites and blueschists in an oblique subduction setting: northeastern Venezuela. *Geology* 18, 950–953.

Backus, G., 1962. Long-wave elastic anisotropy produced by horizontal layering. *J. Geophys. Res.* 70, 3529–3539.

Barruol, G., Hoffmann, R., 1999. Upper mantle anisotropy beneath the geoscope stations. *J. Geophys. Res.* 104, 10,757–10,773.

Blackman, D., Kendall, J.-M., Dawson, P.R., Wenk, H.-R., Boyce, D., Phipps Morgan, J., 1996. Teleseismic imaging of subaxial flow at mid-ocean ridges: travel time effects of anisotropic mineral texture in the mantle. *Geophys. J. Int.* 127, 415–426.

Blackman, D.K., Kendall, J.-M., 2002. Seismic anisotropy of the upper mantle: 2. predictions for current plate boundary flow models. *Geochem., Geophys., Geosyst.* 3 (9,8601). doi:10.1029/2001GC000247.

Buttles, J., Olson, P., 1998. A laboratory model of subduction zone anisotropy. *Earth Planet. Sci. Lett.* 164, 245–262.

Crampin, S., 1984. Effective elastic-constants for wave propagation through cracked solids. *Geophys. J. R. Astron. Soc.* 76, 135–145.

Crampin, S., Booth, B.C., 1985. Shear-wave polarizations near North Anatolian fault, ii, interpretation in term of crack-induced anisotropy. *Geophys. J. R. Astron. Soc.* 83, 75–92.

DeMets, C., Gordon, R.G., Argus, D.F., Stein, S., 1990. Current plate motions. *Geophys. J. Int.* 101, 425–478.

Fischer, K., Wiens, D.A., 1996. The depth distribution of mantle anisotropy beneath the Tonga subduction zone. *Earth Planet. Sci. Lett.* 101 (8), 15987–16002.

Fouch, M.J., Fischer, K.M., 1996. Mantle anisotropy beneath Northwest Pacific subduction zones. *J. Geophys. Res.* 101, 15,987–16,002.

Girardin, N., Gaulon, R., 1983. Microseismicity and stresses in the Lesser Antilles dipping seismic zone. *Earth Planet. Sci. Lett.* 99, 340–348.

Giunta, G., Beccaluva, L., Siena, F., 2006. Caribbean Plate margin evolution: constraints and current problems. *Geologica Acta* 4 (1–2), 265–277.

Gledhill, K., Stuart, G., 1996. Seismic anisotropy in the fore-arc region of the Hikurangi subduction zone, New Zealand. *Phys. Earth Planet. Inter.* 95, 211–225.

Holtzman, B.K., Kohlstedt, D.L., Zimmerman, M.E., Heidelbach, F., Hiraga, T., Hustofo, J., 2003. Melt segregation and strain partitioning: implications for seismic anisotropy and mantle flow. *Science* 301 (5637), 1227–1230.

Jordan, T.H., 1975. The present-day motions of the Caribbean plate. *J. Geophys. Res.* 80, 4433–4439.

Jung, H., Karato, S., 2001. Water-transitions in olivine. *Science* 293, 1460–1463.

Kendall, J.-M., 1994. Teleseismic arrivals at a mid-ocean ridge: effects of mantle melt and anisotropy. *Geophys. Res. Lett.* 21, 301–304.

Kendall, J.-M., Stuart, G.W., Ebinger, C.J., Bastow, I., Keir, D., 2005. Magma assisted rifting in Ethiopia. *Nature* 433, 146–148.

Kneller, E., van Keken, P.E., Karato, S., Park, J., 2005. B-type olivine fabric in the mantle wedge: insights from high-resolution non-Newtonian subduction zone models. *Earth Planet. Sci. Lett.* 237, 781–797.

Lloyd, D., Kendall, J.-M., 2005. Petrofabric derived seismic properties of a mylonitic quartz simple shear zone: implications for seismic reflection profiling. *Petrophys. Prop. Cryst. Rocks* 240, 75–94.

Long, M., van der Hilst, R., 2006. Shear wave splitting from local events beneath the Ryukyu arc: trench-parallel anisotropy in the mantle wedge. *Phys. Earth Planet. Inter.* 155, 300–312.

Lowman, J.P., Piñero-Feliciangeli, L.T., Kendall, J.-M., Shahnas, M.H., 2007. Influence of convergent plate boundaries on upper mantle flow and implications for seismic anisotropy. *Geochem., Geophys., Geosyst.* 8 (Q08007). doi:10.1029/2007GC001627.

Mainprice, D., Barruol, G., Ben Ismail, W., 2000. The seismic anisotropy of the Earth's mantle: from single crystal to polycrystal. *Earth's Deep Inter.* 117 (117), 237–264.

Masson, D.G., Scanlon, K.M., 1991. Neotectonic setting of Puerto Rico. *Geol. Soc. Amer. Bull.* 103 (1), 144–154.

Meschede, M., Frisch, W., 1998. A plate-tectonic model for the Mesozoic and Early Cenozoic history of the Caribbean world. *Tectonophysics* 296, 269–291.

Morley, A., Stuart, G.W., Kendall, J.M., Reyners, M., 2006. Mantle wedge anisotropy in the Hikurangi subduction zone, Central North Island, New Zealand. *Geophys. Res. Lett.* 33 (L05301). doi:10.1029/2005GL024569.

Nakajima, J., Shimizu, J., Hori, S., Hasegawa, A., 2006. Shear-wave splitting beneath the southwestern Kurile arc and northeastern Japan arc: a new insight into mantle return flow. *Geophys. Res. Lett.* 33.

Park, J., Levin, V., 2002. Seismic anisotropy: tracing plate dynamics in the mantle. *Science* 296, 485–489.

Peyton, V., Levin, V., Park, J., Brandon, M., Lees, J., Gordeev, E., Ozerov, A., 2001. Mantle flow at a slab edge: seismic anisotropy in the Kamchatka region. *J. Geophys. Res.* 28, 379–382.

Pindell, J., 1985. Alleghenian reconstruction and the subsequent evolution of the Gulf of Mexico and the Caribbean Sea. *Tectonics* 3, 133–156.

Pindell, J., Barret, S.F., 1990. Geological evolution of the Caribbean region: a plate tectonic perspective. *Geol. Soc. Amer. Bull.* 4, 1–39.

Protti, M., Gündel, F., MacNally, K., 1994. The geometry of the Wadati–Benioff zone under southern Central America and its tectonic significance: results from a high-resolution local seismographic network. *Phys. Earth Planet. Inter.* 84, 271–287.

Russo, R.M., Silver, P.G., 1994. Trench-parallel flow beneath the Nazca plate from seismic anisotropy. *Science* 263, 1105–1111.

Russo, R.M., Speed, R.C., Okal, E.A., Shepherd, J.B., Rowley, K.C., 1993. Seismicity and tectonics of the Southeastern Caribbean. *J. Geophys. Res.* 98, 14,299–14,319.

Russo, R.M., Silver, P.G., Franke, M., Ambeh, W.B., James, D.E., 1996. Shear-wave splitting in northeast Venezuela, Trinidad, and the eastern Caribbean. *Phys. Earth Planet. Inter.* 95, 251–275.

Savage, M.K., 1999. Seismic anisotropy and mantle deformation: what we have learned from shear wave splitting? *Rev. Geophys.* 37, 65–106.

Shih, X.R., Schneider, J.F., Meyer, R.P., 1991. Polarities of P and S waves, and shear wave splitting observed from the Bucaramanga Nest, Colombia. *J. Geophys. Res.* 96, 12,069–12,082.

Silver, P., Chan, W., 1991. Shear wave splitting and subcontinental mantle deformation. *J. Geophys. Res.* 96, 16,429–16,454.

Silver, P., Savage, M., 1994. The interpretation of shear-wave splitting parameters in the presence of two anisotropic layers. *Geophys. J. Int.* 119, 949–963.

- Silver, P.G., 1996. Seismic anisotropy beneath the continent: probing the depths of geology. *Rev. Earth Planet. Sci.* 24, 385–432.
- Stein, S., DeMets, C., Gordon, R., Brodholt, J., Engeln, J.F., Wiens, D.A., Argus, D., Lundgren, P., Stein, C., Woods, D.F., 1988. A test of alternative Caribbean plate relative motion models. *J. Geophys. Res.* 93, 3041–3050.
- Taboada, A., Rivera, L.A., Fuenzalida, A., Cisternas, A., Philip, H., Biijwaard, H., Olaya, J., Rivera, C., 2000. Geodynamic of the northern Andes: subductions and intracontinental deformation (Colombia). *Tectonophysics* 19 (5), 787–813.
- Tommasi, A., Mainprice, D., Cordier, P., Thoraval, C., Couvy, H., 2004. Strain-induced seismic anisotropy of wadsleyite polycrystals and flow patterns in the mantle transition zone. *J. Geophys. Res.* 109 (B12405). doi:10.1029/2004JB003158.
- VanDecar, J.C., Russo, R.M., James, D.E., Ambeh, W.B., Franke, M., 2001. Aseismic continuation of the Lesser Antilles slab beneath continental South America. *J. Geophys. Res.* 75–78.
- Van der Hilst, R., 1990. Tomography with P, PP and PP delay-time data and the three-dimensional mantle structure below the Caribbean region. *Geol. Ultraiectina* 67.
- Vinnik, L.P., Makeyeva, L.I., Milev, A., Usenko, A.Y., 1992. Global patterns of azimuthal anisotropy and deformations in the continental mantle. *Geophys. J. Int.* 111, 433–447.
- Vinnik, P.G., Farra, V., Romanovicz, B., 1989. Azimuthal anisotropy in the earth from observations of SKS at geoscope and NARS broadband stations. *Bull. Seismol. Soc. Am.* 79, 1542–1558.
- Wadge, G., Shepherd, J.B., 1984. Segmentation of the lesser Antilles subduction zone. *Earth Planet. Sci. Lett.* 71, 297–304.
- Wolfe, C.J., Silver, P.G., 1998. Seismic anisotropy of oceanic upper mantle: Shear-wave splitting observations and methodologies. *J. Geophys. Res.* 103, 749–771.